Dependence of the RINGSS weight on the star color

Authors:*A. Tokovinin*
Version: 1
Date: 2021-05-11
File: prj/smass/doc/polyweight.tex

1 Introduction: RINGSS spectral response

The response of the RINGSS instrument (its weighting functions, WFs) depends on the color of the light source, star. This dependence is studied here to decide on the strategy of selecting stars and accounting of their colors in the data reduction. This strategy depends on the filter and detector response: for narrow filters the dependence on color is smaller. The RINGSS instrument is based on the ZWO ASI290M camera and Celestron Nexstar 5SE 5-inch telescope.

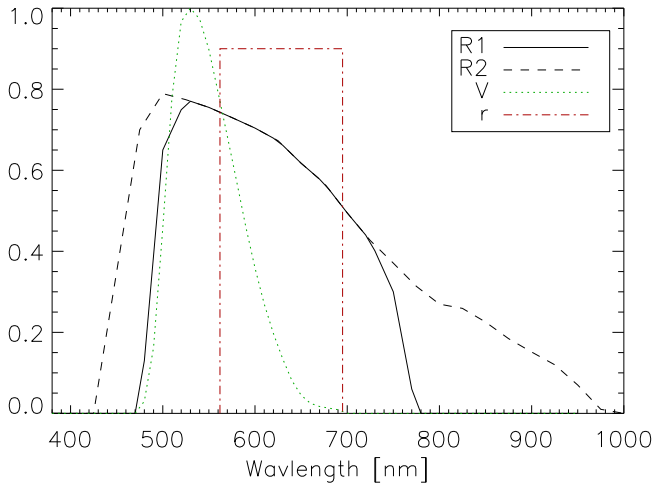

Figure 1: Spectral response of the RINGSS camera and filters in the R1 and R2 configurations. The curves of the photometric V band (dashed line) and the SDSS r' filter (dash-dot) are over-plotted.

Figure 1 plots the spectral response of RINGSS with two filters. R1 is the nominal configuration with the Thorlabs FES0750 short-pass filter that cuts wavelengths longer than 750 nm and also has a cutoff below 500 nm. The R2 configuration uses a yellow glass filter that only cuts wavelengths below ∼450 nm. The filter transmission, multiplied by the QE of the camera, is listed in the text files `quedata3.txt` and `qedata.txt`, respectively. For comparison, the rectangular transmission curve of the SDSS r' Astrodon filter (562-695 nm) is shown. Its 133-nm bandpass would reduce the flux compared to R1, although the sensitivity to the star color will be even less. The study below uses the nominal response curve R1.

2 Stellar colors

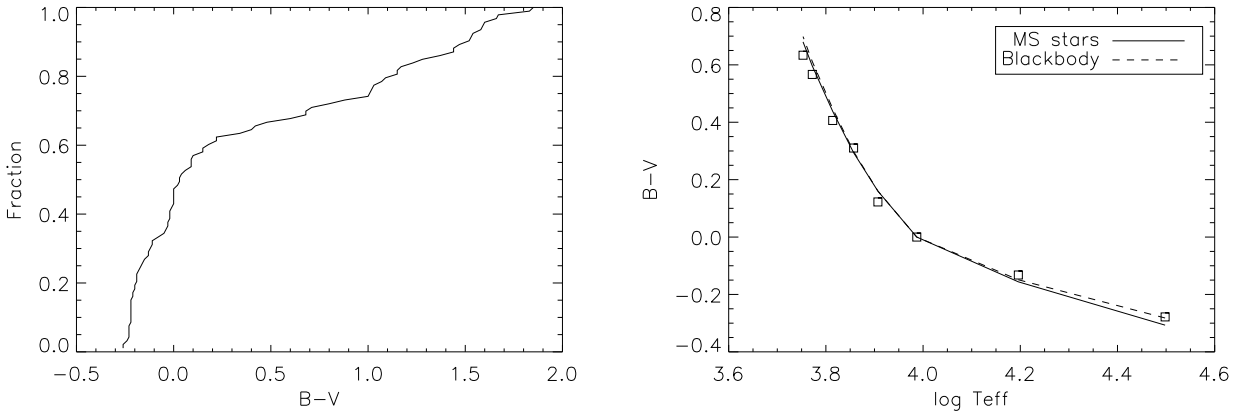

Figure 2: **Left:** Cumulative distribution of $B-V$ colors of 93 stars brighter than $V=2.5$ mag. **Right:** Relation between effective temperature and $B-V$ color for black body radiation (dashed line) and main-sequence stars (solid line and squares).

The left panel of Fig. 2 shows the cumulative distribution of the $B-V$ colors of 93 stars brighter than $V=2.5$ mag selected from the HR catalog (Vizier Catalog V/50). One sees that blue stars dominate, 60% have $B-V<0.2$; the remaining red stars have a wide distribution of the $B-V$ colors. Thus, there is enough bright blue stars (even after rejecting the binaries) to ensure the full sky coverage.

The spectral energy distribution of stars is similar to the black-body spectrum. However, calculation of the $B-V$ colors using the nominal reaction curves from Table 2 of M. Bessell, 1990, PASP, 110, 1181, and the effective temperature of main-sequence stars reveals a systematic difference with the actual $B-V$ colors as tabulated by Mamajek & Pecaut (2013). A much better black-body approximation uses the *color temperature* T_c adjusted to mimic the spectral slope in the B,V region, instead of the *effective temperature* T_e that describes the total energy output. Those temperatures are similar, but not equal.

The code `checksed.pro` computes the $B-V$ colors for a range of black-body spectra with T_c from 3000 K to 30,000 K. I found that the inverse temperature and color are well approximated by the linear relation

$$1/T_c = 9.791\,10^{-5} + 0.000156 * (B-V). \tag{1}$$

The right panel of Fig. 2 plots in solid line the relation between T_e and $B-V$ for main-sequence stars of spectral types from B0V to G5V using the MP13 table. The dashed line plots the black-body color indices using the color temperature from (1). As this approximation is good, the lines nearly coincide. The squares show the $B-V$ colors computed from the true spectral energy distribution of the stars (data used in MASS and provided by V. Kornilov). The agreement justifies the use of the black-body spectra with the color temperature according to (1) as approximations of the real stellar spectra. So, the following study uses the black-body spectra with T_c computed from the $B-V$ colors and the RINGSS response curve R1.

3 Dependence of the WFs on the $B-V$ color

The code `polyweight.pro` computes the WFs for the nominal RINGSS instrument with the spectral response R1 and for propagation distances of 0.5, 1, 2,... 16 km. The $B-V$ colors of -0.2, 0, 0.2, 1., and 1.5 are assumed. The WFs for $B-V=0$ (spectral type A0) is taken as a reference, and the remaining WFs are compared to it. The calculation is done for angular frequencies m from 1 to 20 using the `aweight3.pro` engine. The WF for $m=0$ corresponds to the differential sector motion.

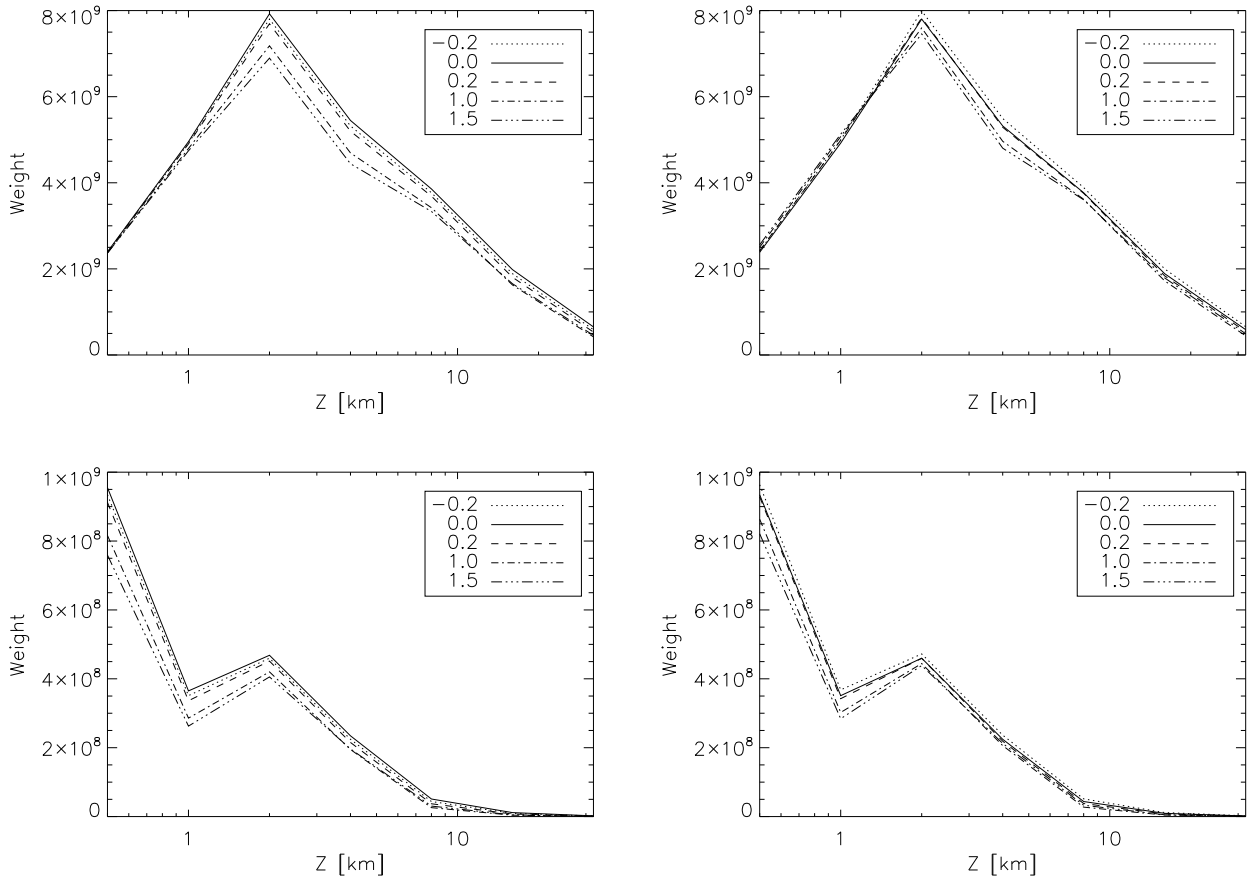

Figure 3: The WFs for $m=5$ (top row) and $m=10$ (bottom row) for stars of different $B-V$ colors (see the legend). The left-hand plots are the raw WFs, the right-hand plots are scaled in proportion to λ_0.

The table below shows the response-weighted effective wavelengths λ_0 for the 5 colors:

B-V	-0.2	0	0.2	1.0	1.5
Lambda0	600.1	605.2	610.7	634.7	649.0

The differential sector motion is achromatic. However, the WF for $m=0$ expresses this motion in the λ_0/D (rather than angular) units. Scaling these WFs in proportion to λ_0^2 removes the color dependence, as readily verified by the explicit calculation.

The scintillation strength generally decreases with increasing wavelength. This is seen in the left panels of Fig. 3, where the computed WFs are plotted for $m = 5$ and $m = 10$. In the right panels, the WFs are multiplied by $\lambda_0/605$ to reduce the color dependence.

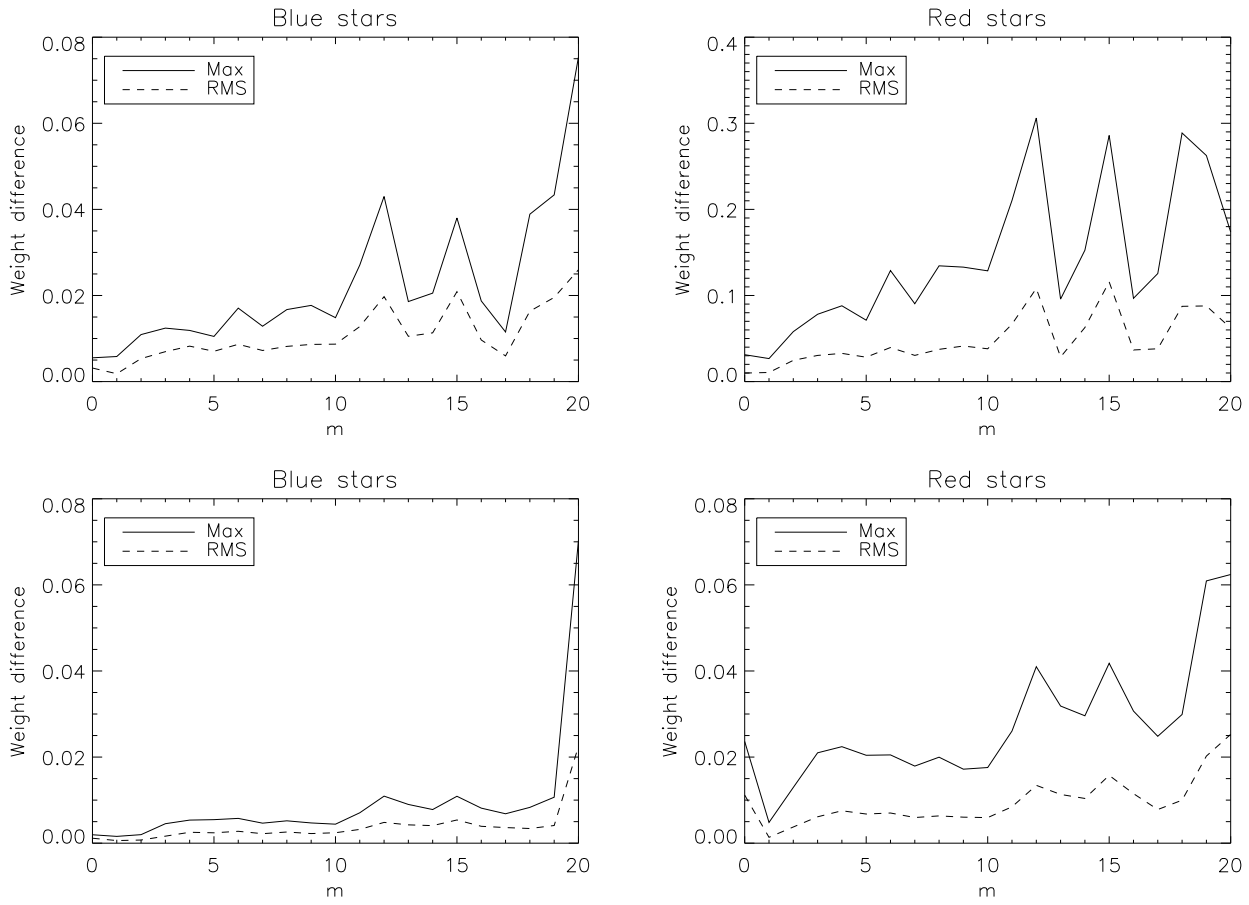

Figure 4: Top row: the maximum and rms difference between the scaled WFs and the WFs for A0V spectral type (normalized by the WF maximum over z) as a function of m. Left: for $B-V$ of -0.2 and 0.2, right: for $B-V$ of 1.0 and 1.5. Bottom row: same for the WF correction via slope.

Figure 4 (top) gives a quantitative measure of the quality of the wavelength-scaled WFs in comparison to the reference WF for A0V ($B-V=0$). For blue stars, the difference (normalized by the peak WF value) is small even without any scaling, and with the scaling it is even less (under 2% rms and 8% maximum). For the red stars (right panel), the scaling does not work as well, but it is still acceptable (rms mostly under 5%). The turbulence profile restoration relies mostly on the signals with $m < 10$, where the scaling works better.

The bottom row of Fig. 4 quantifies the alternative correction strategy where we assume that at each (m, z) the WF depends on the $B-V$ linearly. The slope is just a difference between the WFs computed for $B-V$ of 1 and 0. We need to compute and store two arrays, WFs and slopes. However, the resulting approximation is now much better even for the red stars (by definition, it is perfect for $B-V=1$). In a plot similar to Fig. 3, right, the corrected WF curves practically coincide.

4 Conclusion

This study answers the important practical question: is it necessary to compute a library of WFs for different spectral types, as done in MASS? The answer is negative: we can use the WFs computed for the spectral type A0V and apply small corrections depending on the star $B-V$ color. These corrections (i.e. λ_0) can be established separately, given the instrument response.

An alternative strategy (compute the reference WFs for $B-V$ of 0 and 1 and assume their linear dependence on the color) works even better, at a cost of doubling the WF calculation time.

Another important practical recommendation is to select the stars of blue color, whenever possible. Blue stars dominate, so this choice should be possible.